Free-Surface Turbulence and Mass Transfer in a Channel Flow

Aldo Tamburrino
Water Resources and Environmental Division, Dept. of Civil Engineering, University of Chile, Casilla 228-3, Santiago, Chile

John S. Gulliver
St. Anthony Falls Laboratory, Dept. of Civil Engineering, University of Minnesota, Minneapolis, MN 55455

Free-surface turbulence in a fully developed, open-channel flow was measured for Reynolds numbers of 8,500–45,000. An analysis method of the 2-D divergence on the free surface has been developed to extract Hanratty's β values, or the velocity gradient into the free surface, from these measurements. Hanratty's β is the parameter that relates most directly to the turbulence effect on the liquid-film coefficient. Its measurement is a direct measurement of surface renewal. The spatial scales of β were 3 to 5 times smaller than those of the large upwelling events (boils) normally identified as surface renewal. The hypothesis is that the large upwelling events do not have the high-vorticity gradients associated with large β values. Instead, the locations of high-vorticity gradients on the free surface will also create the divergence required for high β values, occurring at the edges of a large upwelling event. Because the β frequency spectrum has properties to characterize the liquid-film coefficient, it was normalized to be determined from its maximum value, the wave number of this maximum value, and a shape factor used to scale the frequency. Measurements of the liquid-film coefficient from prior studies were also used to characterize the liquid-film coefficient by measured β values for this nonsheared surface. The larger β scales predominantly influence the liquid-film coefficient, in contrast to a previous study of a shear-free surface published by McCready et al. in 1986, where all β frequencies were equally important. Generally, higher frequency turbulence is more significant at a sheared water surface than at a water surface with minimal shear stress.

Introduction

Quantification of mass transfer across gas–liquid interfaces has evolved parallel to quantification of fluid flows. For most chemicals, where flux is controlled by resistance on the liquid side of the interface, the mass flux (F) per unit area can be expressed as

$$F = K\Delta C \tag{1}$$

where ΔC is the concentration difference between the bulk of the liquid and the interface, and K is the liquid film coefficient. In turbulent flows, K is usually characterized as some power-law function of the Reynolds and Schmidt numbers.

The earliest and simplest model for interfacial mass transfer is the film theory presented in 1904 by Nernst (Cussler, 1984, p. 282). It assumes that a stagnant film exists very near the interface. The mass flux across the film is by molecular diffusion alone. Because molecular diffusion is a much slower process than turbulent diffusion, the resistance to mass transfer is localized mainly in the film. Due to the steady uniform laminar flow in the film region, the gradient of concentration is linear, and a relation between the liquid film coefficient K, the molecular diffusivity D, and the film thickness ℓ_f is found

$$K = \frac{D}{\ell_f} \tag{2}$$

Correspondence concerning this article should be addressed to J. S. Gulliver.

In this model, the hydrodynamics of the flow is characterized by ℓ_f, a parameter that remains unknown, but is closely correlated to the thickness of the concentration boundary layer. The primary difficulty with Eq. 2 is that ℓ_f is not constant, but is a function of time, space, and diffusivity in a turbulent flow field.

Since Eq. 2 is difficult to apply, further theories were proposed to estimate ℓ_f. Higbie (1935) presented the "penetration" model that was improved by Dankwerts' (1951) "renewal" model. These are basically unsteady models, where the film thickness is reduced to zero by turbulent eddies coming from the bulk of the fluid at prescribed frequencies (Gulliver, 1991). The thickness of the film is assumed larger than the depth that can be penetrated by molecular diffusion during the film lifetime. Thus, much of the mass transfer is assumed to occur in patches of the free surface during very short periods of time. The difficulty with the renewal theories is that they are conceptual, and are not directly related to near-interface turbulence. Therefore, the measurements of "surface renewal eddies" (Davies and Khan, 1965; Davies and Lozano, 1984; Rashidi and Banerjee, 1988; Gulliver and Halverson, 1989; Komori et al., 1989, 1990; Banerjee, 1991; Komori, 1991) are difficult to correlate with the liquid-film coefficient, because the investigators themselves define what constitutes a surface-renewal eddy.

The primary exceptions to the approach described in the preceding paragraph are the theoretical analyses of Sikar and Hanratty (1970) and Petty (1975), the solid–liquid mass-transfer analysis of Campbell and Hanratty (1982), and the gas–liquid mass-transfer analysis of McCready and Hanratty (1984) and McCready et al. (1986). For example, McCready and Hanratty (1984) adapted the solid wall analysis of Sikar and Hanratty (1970) to develop the boundary-layer equation for concentration in a turbulent flow field near a slip-free interface.

$$\frac{\partial C}{\partial t} + w\frac{\partial \overline{C}}{\partial z} = D\frac{\partial^2 C}{\partial z^2} \tag{3}$$

where C is the instantaneous concentration of the solute, w is the velocity normal to the interface, $\overline{C}$ is the temporal mean solute concentration, and z is the distance from the interface. A series-expansion and order-of-magnitude analysis near the interface resulted in the following relation for vertical velocity

$$w = \beta z \tag{4}$$

where β is the vertical velocity gradient very near the interface. The vertical velocity gradient is a function of time and distance parallel to the interface. This coordinate system moves with the interface, such that $z = 0$ always occurs at the interface.

The importance of the normal velocity gradient, which we will label Hanratty's β, to mass transfer is apparent in Eq. 3. The β parameter is a function of the turbulence in the flow. Continuity (in a control volume that moves vertically) at the free surface gives

$$\beta = \frac{\partial w}{\partial z} = -\left[\frac{\partial u}{\partial x} + \frac{\partial v}{\partial y}\right] \tag{5}$$

Equation 5 gives us a parameter of the flow field, β, that is directly related to interfacial mass transfer via Eqs. 3 and 4. If the free-surface turbulence can be measured or estimated, the conceptual theories become unnecessary.

McCready et al. (1986) solved Eqs. 3, 4, and 5 to characterize K using both a linear and nonlinear approach, as in the work of Campbell and Hanratty (1982), for a solid interface. By means of the linear approach, McCready et al. were able to find an expression for the film thickness, ℓ_f. Most important, they found the dependency of K with parameters that can be obtained from the spectrum of the gradient of the vertical velocity fluctuations. If large frequencies dominate the mass-transfer phenomenon, $K \sim \sqrt{DS_\beta(0)}$, where D is the diffusion coefficient and $S_\beta(0)$ is the frequency spectrum of β, extrapolated to a frequency of zero. If both large and small frequencies are important, K depends on both $\overline{\beta}^2$ and $S_\beta(0)$. In both cases, the dependency of K with the diffusion

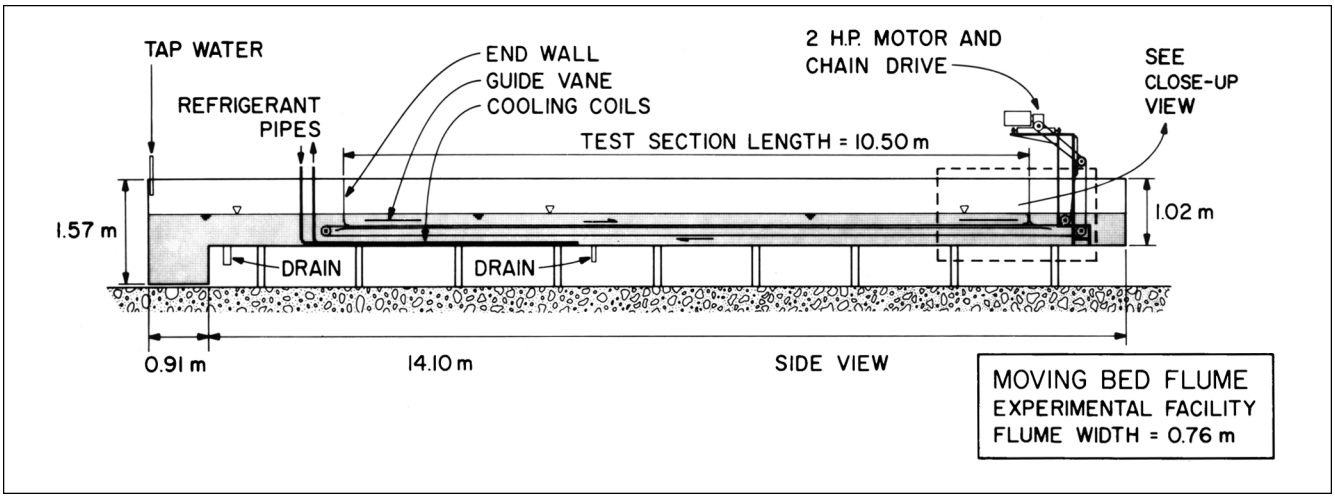

Figure 1. Moving-bed flume (side view).

coefficient agrees with experimental data. In addition, further computations by Back and McCready (1988) have indicated that the fluctuations in K correspond to the low-frequency fluctuations. McCready et al. and Back and McCready assumed, however, that the turbulence measurements of Lau (1980) very near a solid boundary could be used to simulate those of a free-surface generating shear stresses, as long as the free-surface boundary conditions were applied to bring the turbulence to the free surface via Eq. 3. No measurements of free-surface turbulence or β were made.

The free-surface turbulence measurements presented here will test McCready et al.'s hypothesis and be used to infer the parametric relationship between the liquid-film coefficient and free-surface turbulence in an open-channel flow where the turbulence is generated away from the interface.

Measurements of Free-Surface Turbulence

Apparatus

The experiments were performed in the moving-bed flume of the St. Anthony Falls Laboratory, as sketched in Figure 1. It is a channel in which a polyester belt slides on a stainless-steel slider plate. Two transverse vertical metal sheets define the test section, where a recirculating flow is produced by the belt motion. The channel is 15 m long, 0.76 m wide, and 0.69 m deep, with transparent walls made from 0.013-m-thick glass. The belt is 0.71 m wide and can reach a speed of 2 m/s. The moving-bed flume facilitates the acquisition of certain types of data when compared with traditional laboratory flumes. For example, it is possible to set the cross-sectional mean velocity equal to zero at high Reynolds numbers. Then it is not necessary to displace the instrumentation with the flow in order to visualize the structures of the mean flow. This property of the flume will be utilized in the measurements described herein. Further details and a comparison with fixed-bed flume velocity measurements are given in Tamburrino and Gulliver (1992).

Technique

The primary data are obtained by means of time-exposure photographs on the free surface using pliolite particles as tracers. The particles were previously sieved, and only those smaller than 6.2×10^{-5} m (62 microns) were used. Although these particles are considered neutrally buoyant, they float when they are introduced directly into the water surface. During the experiments, the particles were continuously poured on the free surface by means of a feeder located upstream. Adequate illumination was achieved by means of photographic lamps arranged around the flume. At the beginning of the exposure, a flash went off, providing a very short light pulse of high intensity. In this manner, the streak defined by a moving particle is recorded as a "head" followed by a "tail," and the direction of the motion can be determined. The length of the flume covered by each photograph was around 0.75 m.

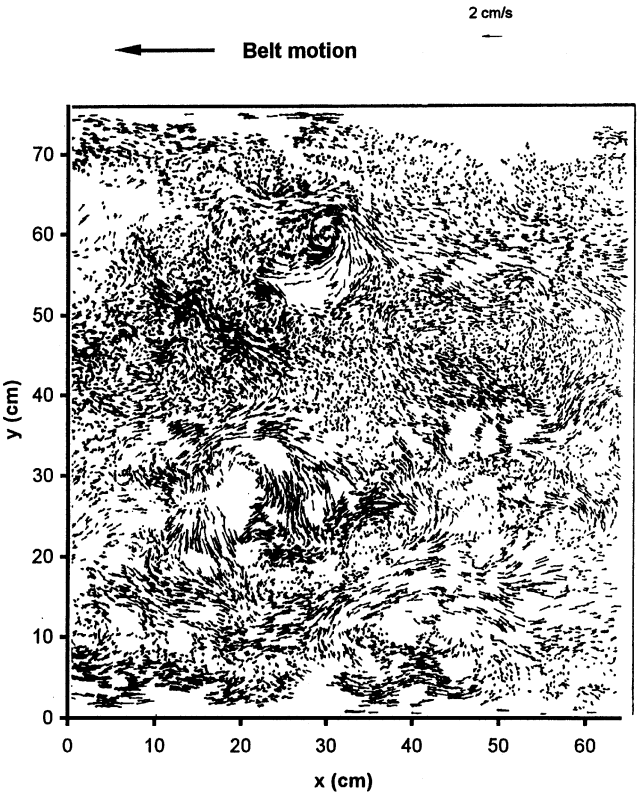

Figure 2. Velocity vector field for Experiment 61 with free-surface mean velocity subtracted.

$H = 0.1263$ m; $W/H = 6.0$; $U_b = 0.183$ m/s; $Re = 22{,}900$; and $Re_* = 1113$.

The photographs obtained in the experiments were enlarged to 0.4×0.5-m (16-in.$\times$20-in.) prints and digitized in order to get the vector field on the free surface (streakline imagery). Digitization was done using a graphic digitizer. The digitized streaks of one photograph are shown in Figure 2. The photographs and their digitization are given for all experimental runs in Tamburrino (1994). The data presented in Figure 2 are randomly distributed in space, but the statistical

Table 1. Experimental Conditions

Exp.	H (m)	U_b (m/s)	u_* (m/s)	U_s (m/s)	W/H	Re	Re_*
61	0.127	0.18	0.0089	0.0220	6.0	22,900	1110
81	0.094	0.19	0.0096	0.0241	8.1	17,200	870
103	0.071	0.66	0.0278	0.0658	10.7	45,500	1920
121	0.061	0.15	0.0083	0.0235	12.5	8,500	510
122	0.060	0.42	0.0202	0.0488	12.7	23,300	1130
123	0.060	0.56	0.0260	0.0596	12.8	31,000	1450

Note: H is channel depth; U_b is the belt velocity; U_s is the mean free-surface velocity; u_* is the channel bottom shear velocity; W/H is the aspect ratio of the flume; $Re = U_b H/\nu$; and $Re_* = u_* H/\nu$.

processing software requires them to be equispaced along the transverse and longitudinal axes. Thus, the original data must be interpolated into the nodes of a grid. Given the characteristics of the experimental data, the kriging method was used because it takes into account the presence of clusters of data and regions with low density of information in the interpolation process (Tamburrino, 1994). Thus, the data were interpolated into the nodes of a 0.005-m $\times$ 0.005-m grid using the kriging method. A summary of the experimental conditions analyzed is given in Table 1.

Measurement uncertainty

A first-order, second-moment uncertainty analysis (Abernathy et al., 1985) was undertaken to quantify measurement uncertainty. The manipulation of the surface streaklines into horizontal velocities assumes that the free surface is perfectly horizontal, with an elevation that is constant over the exposure period, that the streaklines can be digitized accurately, and the interpolation of the streakline data into a square grid will retain sufficient accuracy. Therefore, the potentially significant sources of uncertainty in the measurements are (1) the bias that occurs because the free surface has some overall slope, (2) the precision due to a local curvature in the free surface, (3) the precision due to a vertical motion of the free surface, and (4) the precision introduced in the digitizing and interpolation process.

The details of this uncertainty analysis are given in Tamburrino (1994), and the results are summarized in Table 2. By far, the major source of measurement uncertainty in these experiments was the digitization and interpolation process, with a mean uncertainty in horizontal velocities of 3.6% and a mean uncertainty in β values of between 7.5 and 23%. The uncertainty on the β values is high because this parameter is computed from velocity gradients, which accentuate any measurement uncertainties. If the β values are smoothed over 10^{-4} m^2 (1 cm^2), however, using the eight adjacent β values and the center β values to compute a mean, $\overline{\beta}$, the precision uncertainty of the 10^{-4} m^2 mean value is one-third of the individual uncertainties. Thus, the uncertainty in $\overline{\beta}$ of between 7.5 and 23% results in an uncertainty in $\overline{\beta}$ (over 10^{-4} m^2) of between approximately 2.5 and 7.6%. These smoothed β values are presented in this article. The computed β spectra, however, will not use the smoothed β values, because of the possibility that some information could be missed.

Results

The most important kinematic variable affecting the mass-transfer phenomenon across the free surface is the vertical gradient of the vertical velocity component, as identified by the 2-D divergence in Eq. 5. A high β value can be interpreted as the occurrence of surface renewal.

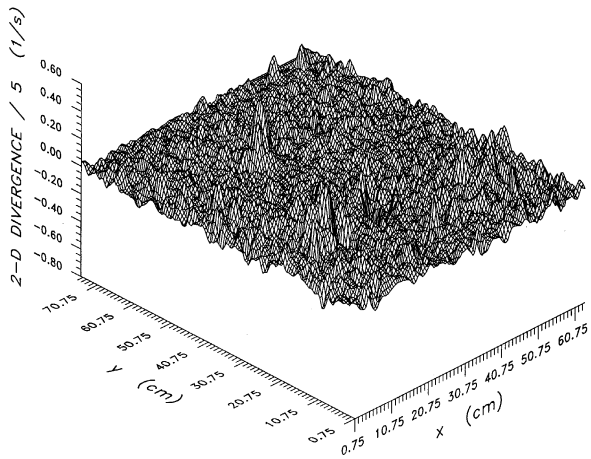

Figure 3. Distribution of smoothed 2-D divergence, Exp. 61.

Vertical velocity gradient

The gradient of the vertical velocity, Hanratty's β, was computed from the interpolated value of u and v replacing the derivatives in Eq. 5 by finite differences. The β values, smoothed over 10^{-4} m^2, are plotted vs. longitudinal and transverse distances for the four representative experiments in Figures 3, 4, 5 and 6. The spatial scales of β seem to be correlated on a wavelength of between 0.02 and 0.03 m. This wavelength is significantly smaller than the 0.06- to 0.15-m scale of the large upwelling events (Imamato and Ishigaki, 1984; Gulliver and Halverson, 1987) in similar flume experiments, which corresponded most closely with channel depth. In fact, a detailed inspection of the data indicates that large β values do not occur at the center of the upwelling regions, but seem to occur at the edges of these boils, where local vortices are formed by the spreading of fluid (Tamburrino, 1994). Thus, the intense horizontal velocity gradients of the smaller vortices created by the upwelling may be responsible for the high values of β, instead of the upwelling itself. This indicates that the long-term, low-intensity upwelling zones traditionally viewed as surface renewal may be less important to mass transfer than short term, high-intensity velocity gradients.

Table 2. Measurement Uncertainties to the 95% Confidence Interval for Computing Horizontal Velocities, u and v, on the Free Surface and Gradient of Vertical Velocity, β, at the Free Surface

Uncertainty Source	Type	Mean Uncertainty in u and v (%)	Mean Uncertainty in β (%)
Overall free-surface slope	Bias	2×10^{-4}	Negligible
Local curvature of free surface	Precision	3×10^{-3}	Negligible
Vertical motion of free surface	Precision	0	0.3–3.8
Digitization and interpolation	Precision	3.6	7.5–23

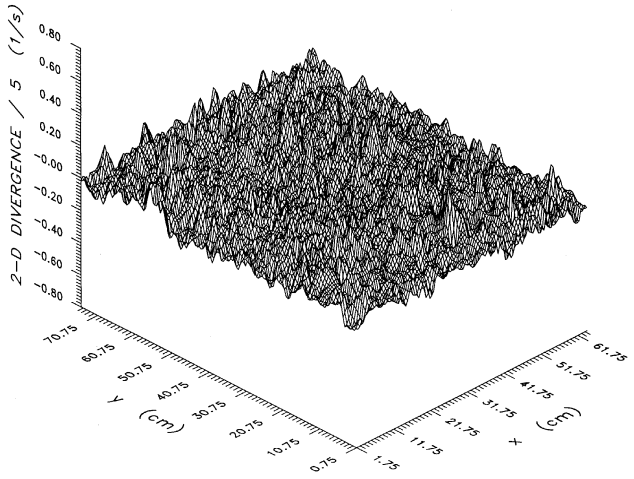

Figure 4. Distribution of the smoothed 2-D divergence, Exp. 81.

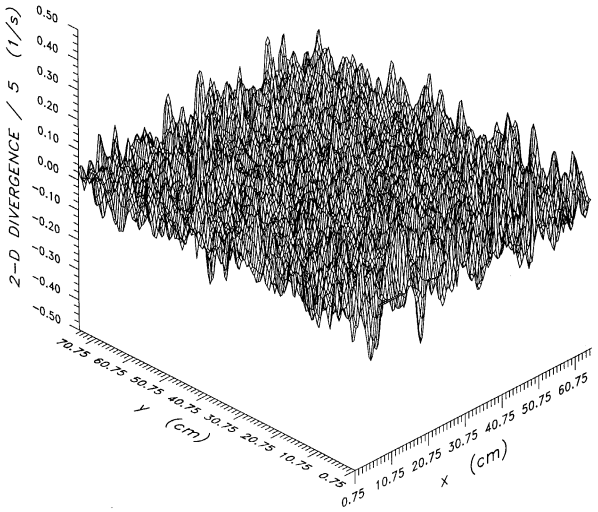

Figure 6. Distribution of the smoothed 2-D divergence, Exp. 121.

The root-mean-square values of Hanratty's β, taken over the entire photographed surface, were computed for each experiment and fit in a linear regression to develop the following empirical relationship (Tamburrino 1994)

$$\sqrt{\overline{\beta^{+2}}} = 0.245 Re_*^{-1.02} \left[\frac{Fr_*}{We_*^{1/2}} \right]^{-0.88} \tag{6}$$

where $\sqrt{\overline{\beta^{+2}}} = \sqrt{\overline{\beta^2}}\, \nu/u_*^2$ is the dimensionless rms value of β, $Re_* = Hu_*/\nu$ is a shear Reynolds number, $Fr_* = u_*/\sqrt{gH}$ is a shear Froude number, and $We_* = \rho H u_*^2/\sigma$ is a shear Weber number, with σ as the surface tension and H as channel depth. This combination of the Froude number and the Weber number results in a Bond of Eötros number, $B_0 = \rho g H^2/\sigma$. Equation 6 is compared with the experimental data in Figure 7. The presence of Froude and Weber numbers arises from the fact that both capillary and gravity forces are the restoring forces that tend to impede the free-surface deformation due to the impinging eddies (Hunt, 1984). The average value of the dynamical trust due to the vertical component of the turbulent fluctuations is given by $\rho\overline{w'^2}$, but close to the free surface, $\overline{w'^2}$ is proportional to u_*^2 (Nezu and Nakagawa, 1993). Thus, the shear velocity is an appropriate choice to represent the dynamics of free-surface deformation.

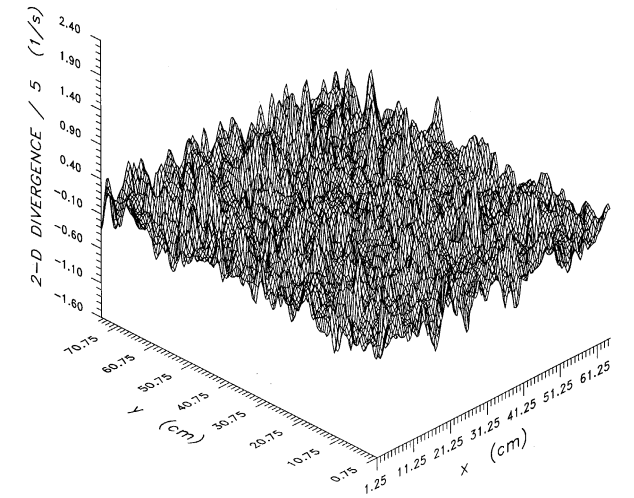

Figure 5. Distribution of the smoothed 2-D divergence, Exp. 103.

Spectra of vertical velocity gradient

The wave-number spectrum of Hanratty's β, S_β, at each longitudinal location for four of the six experiments is presented in Figure 8. The peaks in the spectra occur at wave numbers $\kappa/2\pi$ below 50 m^{-1}, corresponding to wavelengths greater than 0.02 m. The peak at a $\kappa/2\pi$ of 50 m^{-1} corresponding to wavelengths of 0.02 m is especially persistent in these β-spectra. At higher wave numbers, the spectra decreases significantly. At lower wave numbers, the spectra decreases somewhat for flow depths of 0.094 m (Figure 8b) and 0.071 m (Figure 8c), and more quickly at flow depths of 0.06 m (Figure 8d). We believe that the depth of flow limits the scale of surface vorticity, such that the spectra at smaller wave numbers become reduced. No special behavior of the spectra is distinguished across the flume (y-direction). This is in direct contrast to the longitudinal velocity, which was highly correlated in a scale equal to between two and three times the depth, due to large upwelling regions (Tamburrino and Gulliver, 1994). In general, there is no significant change in the dominant frequency of the β-spectra with a change in depth from 0.06 m to 0.12 m or in boundary shear velocity from 0.008 m/s to 0.028 m/s. Apparently, the vertical velocity gradients of the large upwelling zones are overwhelmed by the vertical velocity gradients created by the 2-D vortices on the surface. This can be seen as further evidence that the lower-frequency upwelling zones traditionally identified as surface renewal are not as important for gas transfer as the surface vortices created by the upwelling zones.

The β spectrum of each experiment was averaged and nondimensionalized in the manner of McCready et al. (1986)

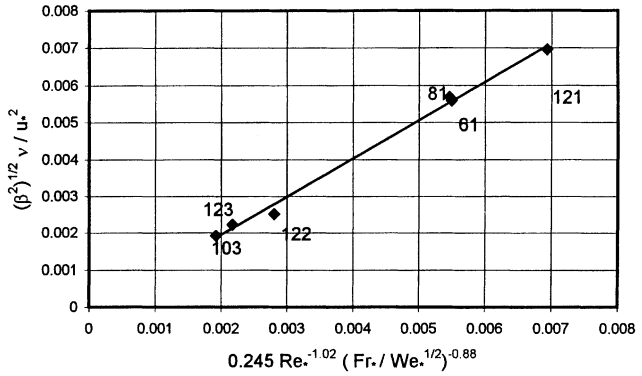

Figure 7. Predicted vs. measured values of the dimensionless, rms vertical velocity gradient for the moving-bed flume.

Experiment number is identified.

and are plotted in Figure 9. Transformation of wave number into frequency is achieved using Taylor's hypothesis (Tennekes and Lumley, 1972) with the mean free-surface velocity, U_s, as the convection velocity (that is, $\kappa\ U_s = \omega$). At the lower frequencies, the β spectra tend to decrease, indicating that the limitation of the flume depth, as described previously, affects the large wavelength of β correlation. The spectra are also somewhat larger than McCready et al.'s, and tend to begin their high ω decrease at a different dimensionless frequency.

The differences between β spectra were rectified through the use of the following relationship

$$S_\beta(\Omega) = \frac{S_{\beta\max}}{1+(\Omega-\Omega_0)^2} \tag{7}$$

where $\Omega = s\omega/\omega_m$, Ω_0 is the nondimensional frequency (Ω) at the peak of the spectrum, s is a shape factor, and ω_m is the mean frequency. For the spectrum given by Eq. 7, the following relationship is satisfied (Tamburrino, 1994)

$$\Omega = \frac{S_{\beta\max}\,\omega}{\overline{\beta^2}}\left[\frac{\pi}{2}+\tan^{-1}\left(\frac{S_{\beta\max}}{S_\beta(0)}-1\right)^{1/2}\right] \tag{8}$$

where the $S_\beta(0)$ term in Eq. 8 is determined by substituting $\Omega = 0$ into Eq. 7. Our experimental data, however, are distributed spatially, such that the wave number is the appropriate spectra abscissa. In terms of wave numbers, Eq. 7 can be written as

$$S_\beta(\kappa) = \frac{a}{1+B\left[\frac{\kappa}{2\pi}-\frac{\kappa_0}{2\pi}\right]^2} \tag{9}$$

Equation 7 has dimensions of s^{-1} and Eq. 9 has dimensions of m s^{-2}. The dimension of a is m s^{-2}, of B it is m^2, and κ has the dimension of m^{-1}. Again using Taylor's hypothesis, Eq. 9 is transformed into Eq. 7 using

$$S_{\beta\max} = \frac{a}{U_s} \tag{10}$$

$$\Omega = \sqrt{B}\,\frac{\kappa}{2\pi} \tag{11}$$

and

$$\Omega_0 = \sqrt{B}\,\frac{\kappa_0}{2\pi} \tag{12}$$

By evaluating the righthand sides of Eqs. 11 and 12, the lefthand sides can be determined without having to compute a mean frequency. Using Eq. 11 and $\kappa\ U_s = \omega$, the following relationship is obtained

$$\frac{s}{\omega_m} = \frac{\sqrt{B}}{U_s 2\pi} \tag{13}$$

A mean frequency depends on the record length, and B is basically determined by how fast the curve defined by Eq. 9 goes down after the plateau. Its determination only requires one to have a portion of the spectrum after the plateau.

In order to make all the spectra collapse into one curve, they were transformed into the parameters $S_\beta(\Omega)/S_{\beta\ \max}$ and $\Omega - \Omega_0$ instead of the normalization $S_\beta(\Omega)/\overline{\beta^2}$ and Ω used in McCready et al. and employed in Figure 9. Fitting of McCready et al.'s spectrum to Eq. 7 gave the following parameters: $S_{\beta\ \max}/\overline{\beta^2} = 14$, $s = 1$, and $\Omega_0 = 0.4$. The value of $S_{\beta\ \max}$ and κ_0 for our data was chosen to provide a best fit of McCready et al.'s data. Our normalization of the data employed by McCready et al. (1986) is presented in Figure 10 together with the spectra corresponding to our experiments. McCready et al.'s transformation from the near wall to a free surface presents more information in the high-frequency range of the spectrum than the data obtained in the moving-bed flume. These data are, however, based on measurements near a solid boundary, rather than at a free surface. It is seen in Figure 10 that all of the normalized spectra collapse onto one curve. It has to be noted that the graph covers only the data with $\Omega > \Omega_0$ because it is not possible to plot negative values in a logarithmic scale.

Figure 10 validates McCready et al.'s assumption that the damping of the gradient of the vertical velocity close to a free surface occurs in a fashion similar to the damping close to a solid wall, although their magnitudes are quite different. In fact, the two flow situations are so different that it is possible that Figure 10 represents a universal spectrum for β. One, however, still needs to determine the parameters $S_{\beta\ \max}$, Ω_0, and Ω for Eqs. 7 and 8 from experiments on near-interface turbulence. The coefficients a, B, and κ_0, from Eqs. 10, 11, and 12, and 13 will enable the estimates of these parameters.

β Spectra vs. mass-transfer coefficient

The linearized theory as developed by Vassiliadou (1985) to relate the spectrum of vertical velocity to the liquid-film coefficient at a free surface will be applied to the measured β-spectra of Figure 10. Although the linearized theory overestimates K, it has been shown to provide the appropriate

parameterization, with a constant fitted to other data, such as that from the disturbed equilibrium measurements of concentration (McCready et al., 1986; Tamburrino, 1994).

Vassiliadou (1985) developed the following expression for the spectrum, S_k^+, of dimensionless liquid-film coefficient, K^+

$$\frac{S_K^+(\Omega)}{K^{+2}} \sim \begin{cases} \dfrac{S_\beta^+(\Omega)}{\Omega_c^2}, & \Omega \le \Omega_c \\ \dfrac{S_\beta^+(\Omega)}{\Omega^2}, & \Omega \ge \Omega_c \end{cases} \tag{14}$$

where the superscript + indicates quantities made dimensionless with the inner variable u_* and ν; Ω_c is a dimensionless cutoff frequency ($\Omega_c = s\omega_c/\omega_m$) that defines the region where the low frequencies dominate; and ω_c is the cutoff frequency. An estimation of ω_c can be obtained by means of an order-of-magnitude analysis of the different terms involved in the linearized diffusion equation (McCready et al., 1986). The cutoff frequency corresponds to the case in which the temporal, advective, and molecular-diffusion terms in Eq. 3 are equally important. For the spectrum given by Eq. 7, this condition is given by (Tamburrino, 1994)

$$\omega_c^+ \cong S_{\beta\,\max}^+ F_\Omega \tag{15}$$

where

$$F_\Omega = \frac{1}{\Omega_c}\left[\tan^{-1}(\Omega_0) - \tan^{-1}(\Omega_0 - \Omega_c)\right] + \frac{1}{\Omega_0^2+1}\left\{\frac{1}{2}\ln\left[(\Omega_0-\Omega_c)^2+1\right] - \ln(\Omega_c)\right\} + \frac{\Omega_0}{\Omega_0^2+1}\left[\frac{\pi}{2} + \tan^{-1}(\Omega_0-\Omega_c)\right] \tag{16}$$

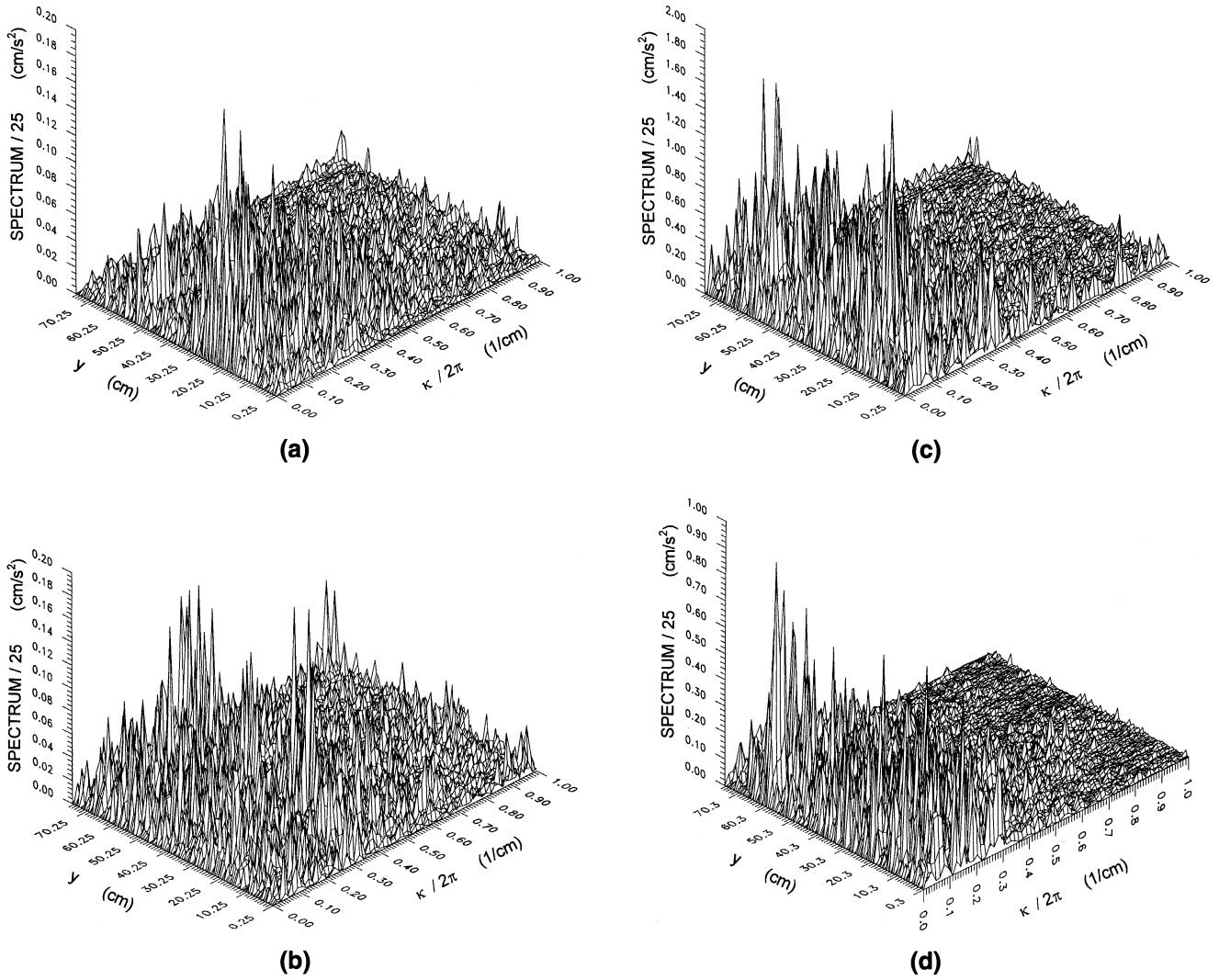

Figure 8. Spectrum of the vertical velocity gradient: (a) Exp. 61; (b) Exp. 81; (c) Exp. 103; and (d) Exp. 122.

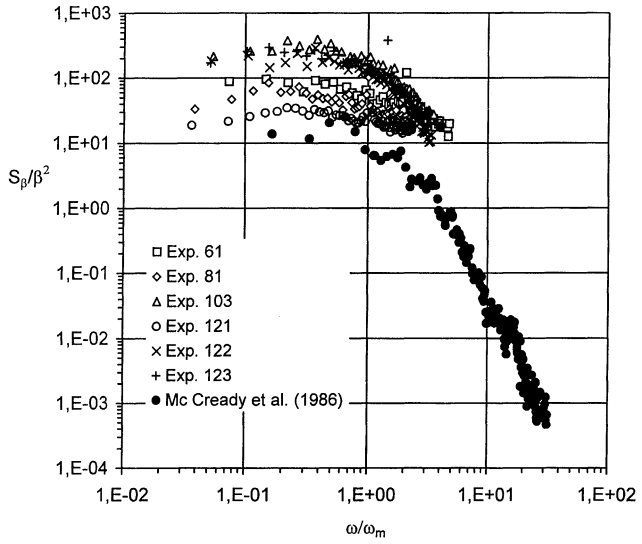

Figure 9. Normalized spectra of Hanratty's β: study vs. spectrum used by McCready et al. (1986) in their computations.

The cutoff frequency ω_c^+ may also be related to the mass-transfer coefficient (Vassiliadou, 1985)

$$\omega_c^+ \sim K^{+2}Sc \tag{17}$$

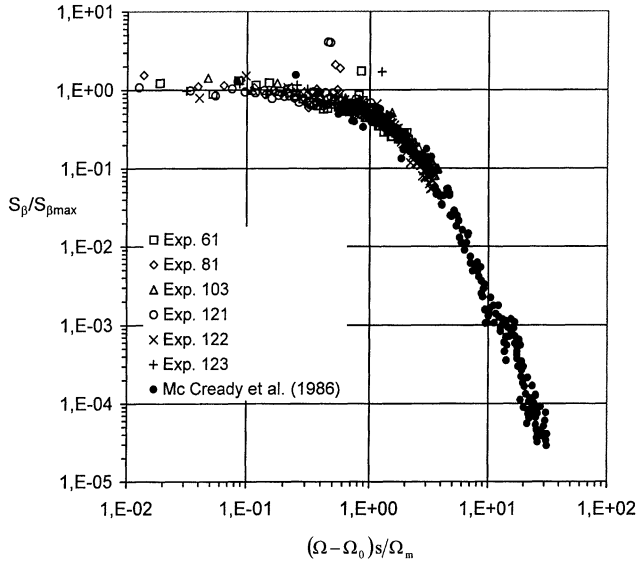

Figure 10. Spectra of Hanratty's β normalized with new parameters.

If Ω_c is large, Eqs. 15, 16 and 17 give

$$K^{+2}Sc \sim \frac{S^+_{\beta\ \max}}{\Omega_c}\left[\frac{\pi}{2}+\tan^{-1}(\Omega_0)\right], \text{ large } \Omega_c \tag{18}$$

which can be reduced to

$$K^+\sqrt{Sc} \sim \overline{(\beta^{+2})}^{1/4} \times \left\{\frac{\pi}{2}+\tan^{-1}\left[\left(\frac{S^+_{\beta\ \max}}{S^+_0(0)}\right)-1\right]^{1/2}\right\}^{-1/4}, \text{ large } \Omega_c \tag{19}$$

Furthermore, if $\Omega_0 \cong 0$ in Eq. 19, then $S^+_{\beta\,\max} \cong S^+_\beta(0)$, and Eq. 19 becomes simply

$$K^+\sqrt{Sc} \sim \overline{(\beta^{+2})}^{1/4} \tag{20}$$

Of course, the value of β^{+2} is still dependent upon $S^+_{\beta\,\max}$, as seen in Eq. 8. With sufficient resolution of data, however, β^{+2} can be measured directly.

McCready et al. (1986) found that their cocurrent air–water mass-transfer experiments follow the behavior indicated by large Ω_c with $\Omega_0 \cong 0$ (Eq. 20). A large Ω_c indicates that there is a higher percentage of small eddies with high energy at the interface. Having $\Omega_0 = 0$ means that the predominant eddies of the flow field are not constrained by the overall length scales. By fitting $S^+_{\beta\,\max}$ and $\overline{\beta^{+2}}$ in their nonlinear model with the gradient of the vertical velocity inferred from measurements near a pipe wall to measurements of $K^+\sqrt{Sc}$ for the cocurrent experiments, they found that their experiments were in the range where $K^+\sqrt{Sc}$ could be described entirely with $\overline{\beta^{+2}}$. They obtained

$$K^+\sqrt{Sc} = 0.71\overline{(\beta^{+2})}^{1/4} \tag{21a}$$

or

$$Sh\sqrt{Sc} = 0.71\overline{(\beta^{+2})}^{1/4} Pe_* \tag{21b}$$

where Sh is a Sherwood number equal to KH/D and Pe_* is a shear Peclet number equal to $u^*\ H/D$. A Sherwood num-

Table 3. Parameters Involved in the β Spectra Computed from Free-Surface Turbulence Measurements in the Moving-Bed Flume

Exp.	$\overline{\beta^{+2}}$	$S^+_{\beta\ \max}$	a (m/s)	B (m^2)	$H\,\kappa_0/(2\pi)$	Ω_0	Ω_c	F_Ω
61	3.119×10^{-5}	2.173×10^{-3}	0.00375	4.5×10^{-4}	0.48	0.084	0.092	3.5171
81	3.222×10^{-5}	1.756×10^{-3}	0.00375	2.6×10^{-4}	0.51	0.087	0.064	3.8696
103	3.698×10^{-6}	1.023×10^{-3}	0.05000	17.1×10^{-4}	0.69	0.405	0.217	2.8556
121	4.842×10^{-5}	1.540×10^{-3}	0.00233	1.8×10^{-4}	0.61	0.134	0.039	4.3976
122	6.324×10^{-6}	1.196×10^{-3}	0.02225	13.8×10^{-4}	0.49	0.308	0.169	3.0640
123	4.946×10^{-6}	1.107×10^{-3}	0.04170	12.7×10^{-4}	0.51	0.303	0.195	2.9254

ber is often preferred (Eq. 21b) to separate the experiments of various length scales (depth), where Eq. 21a will not.

In contrast to the cocurrent experiments of McCready et al. (1986), where shear stress is generated at the air–water interface, the moving-bed flume generates shear at the flume bottom, and the water surface is close to a free-shear boundary. The characterization of Eq. 21 may not apply to our measurements because the intense high-frequency turbulent eddies corresponding to a sheared interface were not present, and our experiments may have had a smaller Ω_c than the data used by McCready et al. At a small Ω_c, Eq. 15 does not reduce to the form of Eq. 21, because both Ω_c and Ω_0 can be small. We will, therefore, test the fit of the data to an equation similar to Eq. 21b, in order to determine whether the assumptions made by McCready et al. can be applied to our flow field.

Another option would be to ignore the assumptions made by McCready et al. in developing Eq. 18. Then, Eqs. 15 and 17 give

$$K^+\sqrt{Sc} \sim S_{\beta\max}^{+1/2} F_\Omega^{1/2} \tag{22}$$

If the experimental data are not characterized by Eq. 21, then it will be fit to Eq. 22, which is more general, but requires the computation of the β-spectrum from measurements. Table 3 presents our computation from the experiments of parameters involved in the precedent equations.

Characterization of mass-transfer coefficient

Disturbed equilibrium measurements of K^+ were made by Gulliver and Halverson (1989) in the same experimental facility and under the same range of depth, bed velocity, and temperature as our free-surface turbulence measurements. Because the flow conditions were not precisely the same, however, the information given in Table 3 was used to develop the following empirical equations to be applied to Gulliver and Halverson's measurements

$$\frac{a\nu}{u_*^3} = 5.53\times10^{-3} Re_*^{-0.48}\left[\frac{Fr_*}{We_*^{1/2}}\right]^{-0.88} \tag{23}$$

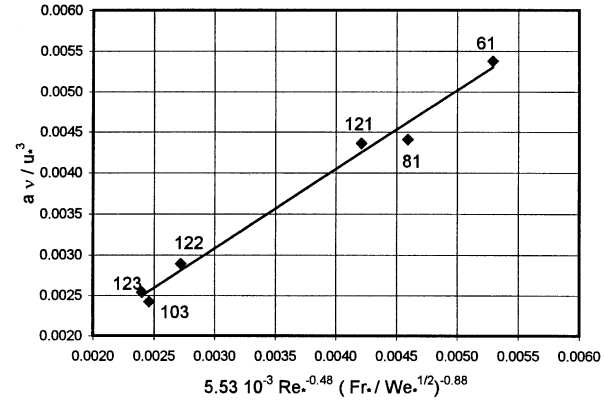

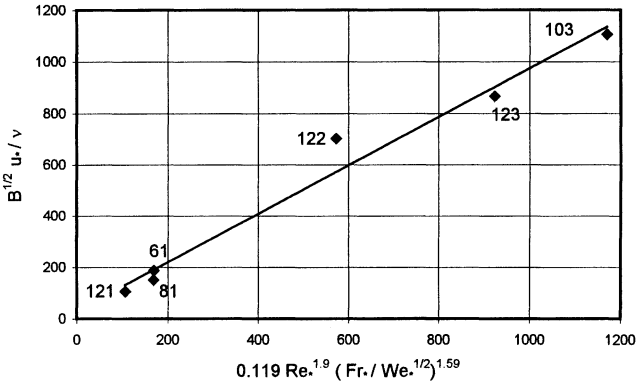

Figure 11. Predicted vs. measured values of parameters used to compute a normalized spectra of the vertical velocity gradient for flumes.

Experiment number is also identified.

$$\frac{\sqrt{Bu_*}}{\nu} = 0.119 Re_*^{1.90}\left[\frac{Fr_*}{We_*^{1/2}}\right]^{-0.59} \tag{24}$$

$$H\frac{\kappa_0}{2\pi} = 0.55 \tag{25}$$

The predicted values from Eqs. 23 and 24 are compared with the experimental data of Table 4 in Figure 11. Equation 25 had a standard deviation of 14.8% when the fitted and measured values were compared.

Table 4. Experimental Research Directly Relating the Liquid-Film Coefficient to Hanratty's β

Research	Data	Condition	Relationship	Comments
Campbell and Hanratty (1982)	Mass-transfer and velocity measurements in a pipe	Flow near a solid wall	$K^+ Sc^{0.7} = 0.237\, S_{\beta\,\max}^{+0.21}$	Coefficient obtained after fitting nonlinear model to experimental data
McCready et al. (1986)	Velocity gradients from measurements in a pipe. K measured in cocurrent current air–water flows	Free-surface cocurrent flow	$K^+ Sc^{0.5} = 0.71\,(\overline{\beta^{+2}})^{0.5}$	Same as before, with free-surface boundary conditions applied to near-wall data
This research	Velocity gradients measured at the free surface. K measured in open-channel flows	Free-surface open-channel flow	$K^+ Sc^{0.5} = 0.24\, S_{\beta\,\max}^{+0.5}$	Functional relationship obtained from linear analysis. Coefficient obtained after fitting linear model with experimental data

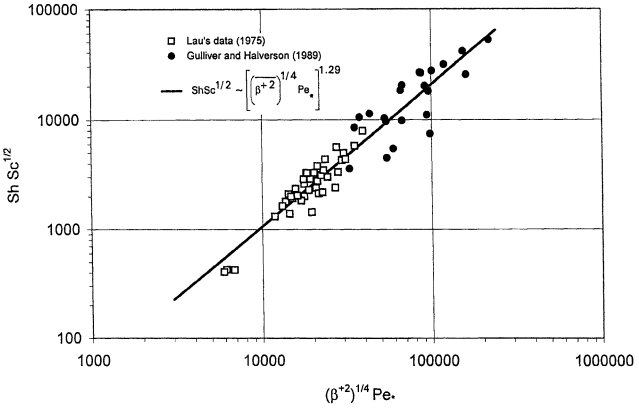

Figure 12. Relationship between $Sh\ Sc^{1/2}$ and $(\beta^{+2})^{1/4} Pe_*$.

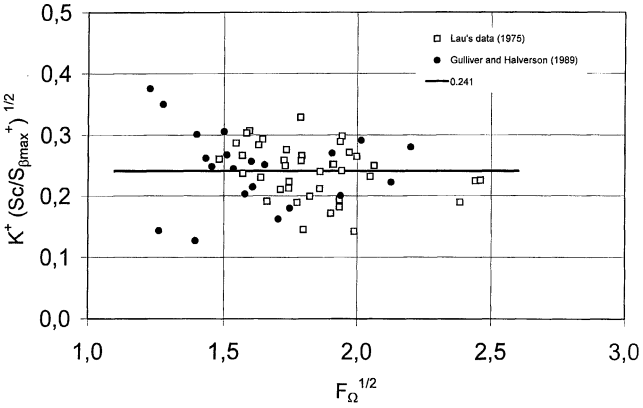

Figure 13. Relationship between $K^+\sqrt{Sc/S_{\beta max}^+}$ and $\sqrt{F_\Omega}$.

Equations 6 and 23 through 25 were also applied to the disturbed equilibrium measurements of Lau (1975) (given in Gulliver and Halverson, 1989) in a different flume. The surface turbulence was also generated by the bottom shear in Lau's experiments, and the flume was sufficiently long (100 m) that the turbulent boundary layer was fully developed over a large portion of the flume.

We first plotted the data of Lau (1975) and Gulliver and Halverson (1989) in a form similar to Eq. 21b, except that a variable power was placed on the righthand side of the equation. The result, given in Figure 12, is best fit by the following equation

$$Sh\sqrt{Sc} \sim \left[\left(\overline{\beta^{+2}}\right)^{1/4} Pe_*\right]^{1.29} \tag{26}$$

Equation 21 would have this characterization be to the first power, instead of the 1.29th power. There are two possibilities for this characterization to the 1.29th power: first, it is possible that Eq. 6, an empirical fit of β data and bulk-flow characteristics in the moving-bed flume, does not apply to Lau's data, which was measured in flows of lower depth; second, it is possible that the assumptions made in arriving at the characterization of Eq. 21 do not apply in the case of the bottom-generated turbulence, that is, that Ω_c is too small, approaching Ω_0, such that the proportionality described by Eq. 22 must be used. Observing the values of Ω_0 and Ω_c in Table 3, we see that Ω_c approaches Ω_0, and the second hypothesis is true.

In a similar manner Eq. 22 with a constant coefficient α becomes

$$K^{+2}\frac{Sc}{S_{\beta max}^+} = \alpha F_\Omega \tag{27}$$

The parameters $S_{\beta max}^+$ and F_Ω were computed using Eqs. 10, 16, and 23 for both sets of data. The results are plotted in Figure 13, with the square root of the lefthand side term of Eq. 27 in the y-axis and $F_\Omega^{1/2}$ in the x-axis. There does not appear to be a dependency of $K^+\sqrt{Sc/S_{\beta max}^+}$ upon $\sqrt{F_\Omega}$ in the range of the reported variables, and the constant α is equal to 0.24. Thus, the mass-transfer coefficient measured by Gulliver and Halverson and by Lau can be represented by

$$K^+\sqrt{Sc} = 0.24\sqrt{S_{\beta max}^+} \tag{28a}$$

or

$$Sh\sqrt{Sc} = 0.24\sqrt{S_{\beta max}^+}\,Pe_* \tag{28b}$$

which is plotted with the data in Figure 14. We believe that this equation is more general than Eq. 26, and has a greater applicability to flow outside the range of those laboratory experiments used to fit the coefficients. It possibly can be used to represent the liquid film coefficient in any flow where turbulence is generated away from the free surface. Equation 28 can, therefore, be seen as a "bottom-turbulence" companion to McCready et al.'s (1986) relationship, Eq. 21, where shear is generated at the interface, and to Campbell and Hanratty's (1982) relation for turbulence near a wall. Additional, and improved, data of the free-surface kinematics and liquid-film coefficient will result in a refinement of the coefficient in Eqs. 21 and 28.

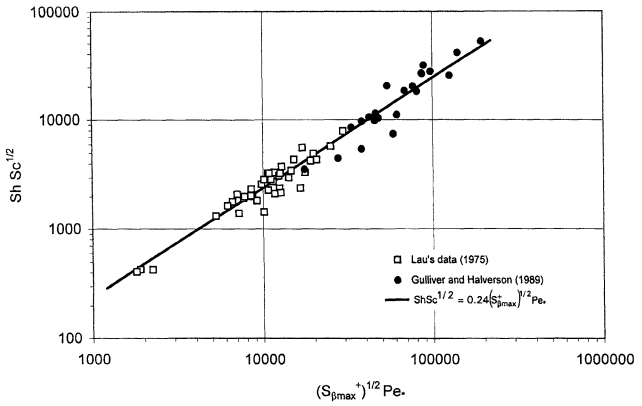

Figure 14. Relationship between $Sh\ S_c^{1/2}$ and $S_{\beta max}^{+1/2} Pe_*$.

Conclusions

The gradient of the vertical velocity at the free surface, Hanratty's β, was computed from the measured spatial distribution of the free-surface turbulence in the flow field. The linear theory of McCready et al. (1986) indicates that the frequency spectrum of β plays an important role in characterizing the mass transport across the gas–liquid interface. Spectra of β computed for different flow conditions can be fitted to a simple expression and is fully defined by three parameters: the spectrum maximum, the frequency at which the maximum occurs, and a shape factor incorporated into the normalized frequency.

Adequate scaling of the measured spectra of β allowed all spectra to collapse into a single curve, including the spectrum computed from a pipe flow, reported by McCready et al. (1986). This validates the assumption made by McCready et al. (1986) that the shape of the β spectrum obtained in a pipe flow can be converted to that for an open-channel flow. This analysis also suggests that the β spectrum scaling developed herein could be universal, in the range of frequencies that are of interest for the mass-transfer phenomenon. If this is true, future research could concentrate on estimating the three scaling parameters for the β-spectrum. The relationship between the dimensionless universal spectra of β and $K^+\sqrt{Sc}$ would then be invariant, where K^+ is the dimensionless liquid-film coefficient and Sc is the Schmidt number.

The upwelling locations identified in many studies as the indicator of surface renewal may not be the locations of high mass transfer. An analysis of the spatial scales of β showed that the distance between peaks and troughs were not on the order of channel depth in the flume. This indicates that high values of β are not a primary result of the large upwellings that come to the surface, which do scale with channel depth. The spatial scales of β are more closely related to the high-velocity gradients of surface vorticity, which can be a consequence of the upwelling due to large upwellings, but are not traditionally identified as a source of surface renewal. This observation needs further study.

The proportionality between the dimensionless terms $K^+\sqrt{Sc}$ and $\sqrt{S^+_{\beta\max}}$, where $S^+_{\beta\max}$ is the dimensionless maximum value of the β spectrum, was obtained for an open channel flow with nearly zero shear at the air–water interface. The linear theory of Vassiliadou (1985) indicates that, for this case, the larger turbulence scales have a significant contribution to mass transfer.

With interfacial shear, McCready et al. (1986) found a proportionality between $K^+\sqrt{Sc}$ and $\left(\overline{\beta^{+2}}\right)^{0.25}$, indicating that both large and small turbulence scales contribute to mass transfer. It is possible that the higher-frequency fluctuations associated with a sheared surface simply are not present at the outer edge of a confined boundary layer (the free surface) without shear stress. This observation corresponds to the results of the attached eddy model (Perry and Marusic, 1995; Marusic, 2001).

Using the results of mass-transfer experiments performed by Gulliver and Halverson (1989) in the same facility used in this research, and by Lau (1975) in a different facility, the following relation was found

$$K^+\sqrt{Sc} = 0.24\sqrt{S^+_{\beta\max}}$$

The research on Hanratty's β and its relation to the mass coefficient are summarized in Table 4.

Acknowledgment

This article is based on work partially supported by the National Science Foundation under Grant No. CES-8615279. Any opinions, findings, and conclusions or recommendations expressed are those of the authors and do not reflect those of the National Science Foundation. The first author also acknowledges the partial financial support given by the Graduate School of the University of Minnesota as a Doctoral Dissertation Special Grant. The authors thank Mr. Joseph Orlins for assisting with data presentation.

Literature Cited

Abernathy, R. B., R. P. Benedict, and R. B. Dowdell, "ASME Measurement Uncertainty," *J. Fluids Eng.*, **107**, 161 (1985).

Back, D. D., and M. S. McCready, "Theoretical Study of Interfacial Transport in Gas-Liquid Flows," *AIChE J.*, **34**, 1789 (1988).

Banerjee, S., "Turbulence/Interface Interaction," *Phase-Interface Phenomenon in Multiphase Flows*, G. F. Hewit, F. Mazinger, and J. R. Riznic, eds., Hemisphere, New York, p. 3 (1991).

Campbell, J. A., and T. J. Hanratty, "Mass Transfer Between a Turbulent Fluid and a Solid Boundary: Linear Theory," *AIChE J.*, **28**, 988 (1982).

Cussler, E. L., *Diffusion. Mass Transfer in Fluid Systems*, Cambridge Univ. Press, New York, p. 282 (1984).

Dankwerts, P. V., "Significance of Liquid-Film Coefficients in Gas Absorption," *Ind. Eng. Chem.*, **43**, 1460 (1951).

Davies, J. T., and W. Khan, "Surface Clearing by Eddies," *Chem. Eng. Sci.*, **20**, 713 (1965).

Davies, J. T., and F. J. Lozano, "Turbulence and Surface Renewal at the Clear Surface in a Stirred Vessel," *AIChE J.*, **30**, 502 (1984).

Gulliver, J. S., "Introduction to Air-Water Mass Transfer," *Air-Water Mass Transfer*, S. C. Wilhelms and J. S. Gulliver, eds., ASCE, New York (1991).

Gulliver, J. S., and M. J. Halverson, "Air-Water Gas Transfer in Open Channels," *Water Resourc. Res.*, **25**, 1783 (1989).

Gulliver, J. S., and M. J. Halverson, "Measurements of Large Streamwise Vortices in an Open-Channel Flow," *Water Resour. Res.*, **23**, 115 (1987).

Higbie, R., "The Rate of Absorption of a Pure Gas into a Still Liquid During Short Periods of Exposure," *AIChE Trans.*, **31**, 365 (1935).

Hunt, J. C. R., "Turbulence Structure and Turbulent Diffusion Near Gas-Liquid Interfaces," *Gas Transfer at Water Surfaces*, W. Brutsaert and G. H. Jirka, eds., Reidel, Dordrecht, The Netherlands, p. 67 (1984).

Imamoto, H., and T. Ishigaki, "Visualization of Longitudinal Eddies in and Open-Channel Flow," *Proc. Int. Symp. on Flow Visualization*, Hemisphere, New York, p. 333 (1984).

Komori, S., "Surface-Renewal Motions and Mass Transfer Across Gas-Liquid Interfaces in Open-Channel Flows," *Phase-Interface Phenomena in Multiphase Flow*, G. H. Hewit, F. Mayinger, and J. R. Riznic, eds., Hemisphere, New York, p. 31 (1991).

Komori, S., R. Nagosa, and Y. Murakami, "Mass Transfer into a Turbulent Liquid Across the Zero-Shear Gas-Liquid Interface," *AIChE J.*, **36**, 957 (1990).

Komori, S., Y. Murakami, and H. Ueda, "The Relationship Between Surface Renewal and Bursting Motions in an Open-Channel Flow," *J. Fluid Mech.*, **203**, 103 (1989).

Kumar, S., and S. Banerjee, "Development and Application of a Hierarchical System for Digital Particle Image Velocimetry to Free-Surface Turbulence," *Phys. Fluids*, **10**(1), 160 (1998).

Lau, K. K., "Study of Turbulent Structure Close to a Wall Using Conditional Sampling Techniques," PhD Thesis, Univ. of Illinois, Urbana (1980).

Lau, Y. L., "An Experimental Investigation of Reaeration in Open Channel Flow," *Prog. Water Technol.*, **7**(3/4), 519 (1975).

Marusic, I., "On the Role of Large-Scale Structures in Wall-Turbulence," *Phys. Fluids*, **13**(3), 734 (2001).

McCready, M. A., E. Vassiliadou, and T. Hanratty, "Computer Simulation of Turbulent Mass Transfer at a Mobile Interface," *AIChE J.*, **32**(7), 1108 (1986).
McCready, M. J., and T. J. Hanratty, "A Comparison of Turbulent Mass Transfer at Gas-Liquid and Solid-Liquid Interfaces," *Gas Transfer at Water Surfaces*, W. Vrutsaert and G. H. Jirka, eds., Reidel, Hingham, MA (1984).
Nezu, I., and H. Nakagawa, *Turbulence in Open Channel Flows*, Balkema, Rotterdam, The Netherlands (1993).
Perry, A. E., and I. Marusic, "A Wall-Wake Model for the Turbulence Structure of Boundary Layers: I. Extension of the Attached Eddy Hypothesis," *J. Fluid Mech.*, **298**, 361 (1995).
Petty, C. A., "A Statistical Theory of Mass Transfer Near Interfaces," *Chem. Eng. Sci.*, **30**, 413 (1975).
Rashidi, M., and S. Banerjee, "Turbulence Structure in Free-Surface Channel Flows," *Phys. Fluids*, **31**(9), 2491 (1988).
Sirkar, K. K., and T. J. Hanratty, "Turbulent Mass Transfer Rates to a Wall for Large Schmidt Numbers to the Velocity Field," *J. Fluid Mech.*, **44**, 598 (1970).
Tamburrino, A., and J. S. Gulliver, "Comparative Flow Characteristics of a Moving-Bed Flume," *Exp. Fluids*, **13**, 289 (1992).
Tamburrino, A., and J. S. Gulliver, "Free-Surface Turbulence Measurements in an Open-Channel Flow," *ASME, FED*, Vol. 181, E. P. Rood and J. Katz, eds., American Society of Mechanical Engineers, New York, p. 103 (1994).
Tamburrino, A., "Free-Surface Kinematics: Measurement and Relation to the Mass Transfer Coefficient in Open Channel Flow," PhD Thesis, Univ. of Minnesota, Minneapolis (1994).
Tennekes, H., and J. L. Lumley, *A First Course in Turbulence*, MIT Press, Cambridge, MA, p. 252 (1972).
Vassiliadou, E., "Turbulent Mass Transfer to a Wall at Large Schmidt Numbers," PhD Thesis, Univ. of Illinois, Urbana (1985).

Manuscript received Dec. 19, 2000, and revision received June 13, 2002.